JACS
JOURNAL OF THE AMERICAN CHEMICAL SOCIETY
Article
pubs.acs.org/JACS

Tuning the Photoresponse in Organic Field-Effect Transistors

Mirella El Gemayel,[†] Matthias Treier,[†] Chiara Musumeci,[†] Chen Li,[‡] Klaus Müllen,[‡] and Paolo Samorì*[,†]

[†]Nanochemistry Laboratory, ISIS-CNRS 7006, Université de Strasbourg, 8 allée Gaspard Monge, 67000 Strasbourg, France
[‡]Max-Planck Institute for Polymer Research, Ackermannweg 10, 55124 Mainz Germany

Supporting Information

ABSTRACT: We report on the fabrication of solution-processed organic phototransistors (OPTs) based on perylenebis(dicarboximide)s (PDIs). We found that the responsivity to the photoillumination depends on the transistor's channel length and that it can be tuned by varying the device geometry. The analysis of different morphologies of the active semiconducting layer revealed that single PDI fibers exhibit the higher photoresponse when compared to more poorly organized films. The highest responsivity value of 4.08 ± 1.65 × 10^5 A/W was achieved on a multifiber-based OPT. These findings represent a step forward toward the use of organic based phototransistors as photosensors.

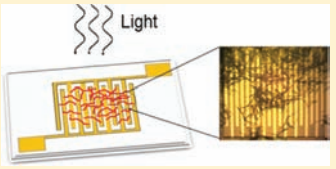

INTRODUCTION

Conjugated organic materials with semiconducting properties have been intensively studied in view of their (opto)electronic applications in a technology relying on low-cost fabrication methods, low processing temperatures, large area coverages and structural flexibility. Among low molecular weight organic semiconductors, perylenebis(dicarboximide)s (PDIs) are the most widely studied and applied active components in optoelectronics due to their relatively strong electron affinities, stability, and easily controllable properties.[1] The electron transporting character of PDI, first demonstrated by Horowitz and co-workers on vacuum-processed films[2] in 1996, has been exploited in the past few years in organic soluble *N,N′*-alkyl substituted PDI (PDI-Cn) derivatives to fabricate organic field-effect transistors (OFETs).[3] Their unique optical properties,[4] also make them excellent candidates as electron accepting building blocks for photovoltaics applications.[5] In particular, their absorption characteristics in the visible region render them appealing as light-sensitive materials for organic phototransistors (OPTs).

In OPTs additional charge carriers are generated in a semiconducting material upon illumination. OPTs are not only interesting device prototypes for investigating opto-electronic properties of a given material with respect to its chemically tailored absorption properties, but they are also promising architectures for realizing photosensors.[6] In addition to charge carrier mobility, threshold voltage and on/off ratio, the key parameters for evaluating the performance of OPTs are (i) the photosensitivity ***P*** defined as

$$P = \frac{I_{light} - I_{dark}}{I_{dark}}$$

with I_{light} and I_{dark} being the drain current under illumination and in dark, respectively, and (ii) the responsivity ***R*** being

$$R = \frac{I_{light} - I_{dark}}{E_{light}} \quad (1)$$

with incident light intensity E_{light} (usually expressed in W/cm^2). While ***P*** provides a measure for the increase in signal upon illumination, ***R*** quantifies the ability of a device to convert light into electric current.[6] OPTs based on PDI derivatives have been reported,[3a,7] and it has been demonstrated that light can be efficiently used as an additional control parameter. However, the key issue remains that responsivity should be as high as possible for efficient light detection. Hitherto, a responsivity of 11000 A/W under monochromatic light with low intensity (1.4 μW/cm^2) has been reported for OPTs based on anthracene crystalline microplates.[8] OPTs based on 6-methyl-anthra[2,3-*b*]benzo[*d*]thiophene microribbon exhibited a responsivity of up to 12000 A/W (30 μW/cm^2).[9] In the former case the high photoresponse as compared to that of the thin film-based devices was attributed to the highly ordered J-type aggregates forming crystalline microplates. In the latter case it was proposed that the possible reasons behind this behavior could be the intrinsic property of the semiconductor and the lifetime of excitons.

Here we demonstrate that the photoresponse of OPTs based on PDI-Cn derivatives **1**−**3** (Figure 1a) can be tuned through device geometry and via self-assembly of PDIs using two different solution processing techniques. In particular we show that the optical responsivity ***R*** is channel length dependent such that it can be increased by several orders of magnitude for any material by careful device geometry optimization.

EXPERIMENTAL METHODS

Device Fabrication. Bottom-gate bottom contact transistors featuring 230 nm thermally grown oxide on n++-doped silicon (Frauenhofer Institute, capacitance 1.5 × 10^{-8} F/cm^2) were used. Each substrate exposes prepatterned interdigitated Au source-drain electro-

Received: December 9, 2011
Published: January 5, 2012

   dx.doi.org/10.1021/ja211515b | *J. Am. Chem.Soc.* 2012, 134, 2429−2433

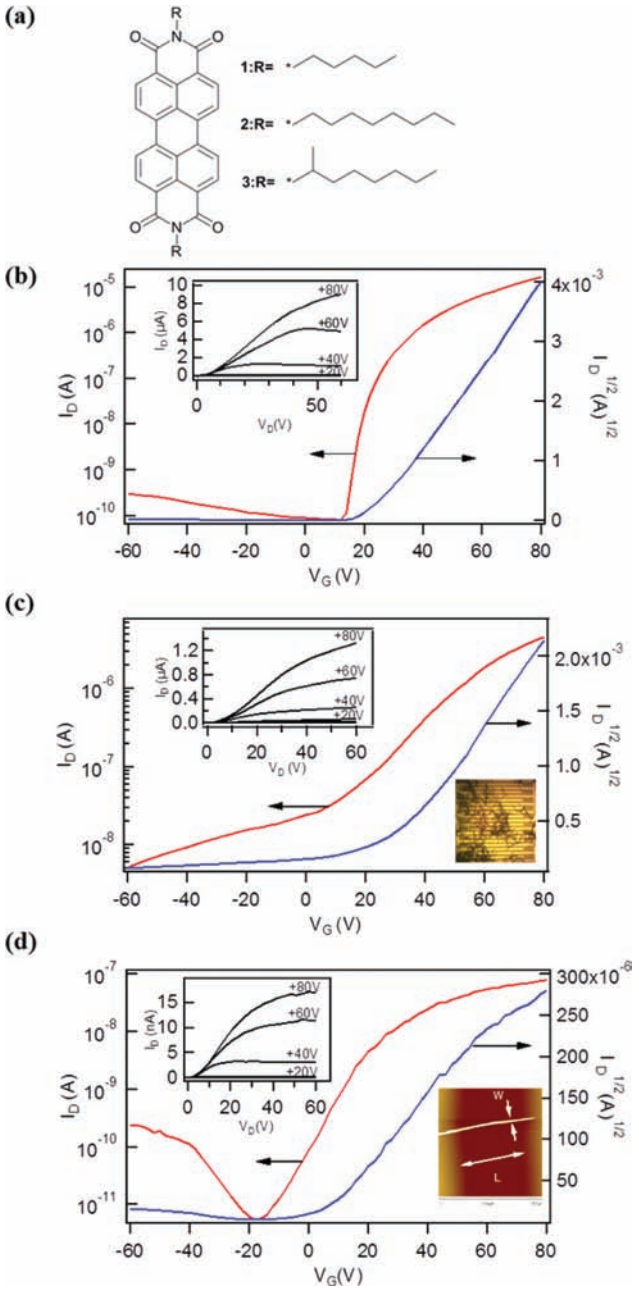

Figure 1. (a) Chemical formulas of the PDI derivatives. Transfer characteristics at V_D = 80 V of OFETs with L = 20 μm of **1** (b) film (*tf-OFET*), and of (c) drop-casted fibers (*multifib-OFET*). Insets: Output characteristics. Optical microscopy image of *multifib-OFET* of **1** (bottom right). (d) Transfer characteristics at V_D = 80 V of *monofib-OFET* of **1** (L = 14 μm). Insets: its output characteristics and its AFM image (bottom right).

des with different channel length (L = 2.5, 5, 10, 20 μm) and constant channel width (W = 10 mm). These substrates were cleaned in an ultrasonic bath of acetone and isopropanol prior to device fabrication.

To improve both the adhesion of the hydrophobic organic semiconductor onto the surface and the charge injection into the organic semiconductor, by reducing the work function, the Au electrodes were treated with self-assembled monolayers (SAMs) of undecanethiol (1 mM). Subsequently, substrates were transferred to a N_2 filled glovebox (O_2 and H_2O content below 8 ppm and 2 ppm, respectively) where the SiO_2 dielectric interface was rendered hydrophobic upon treatment with hexamethyldisilazane (HMDS), followed by thermal annealing at 80 °C for 1 h. Thin films were prepared by spin-coating 60 μL of **1**−**3** solutions (0.25 mg/mL) in chloroform (at 700 rpm for 60 s). Fiber-based devices were prepared by drop-casting onto the HMDS-treated substrate the fibers of **1**−**3** previously formed by solvent-induced precipitation, i.e. by adding methanol into 0.25 mg/mL PDI solution in chloroform at a ratio of 1:5. **1** and **2** (98%) (Sigma Aldrich) were used as purchased, whereas **3** was synthesized as described elsewhere.[10]

Conversely, single-fiber devices based on **1** were fabricated using a bottom-gate top-contact geometry, by first casting SIP preformed fibers on the untreated SiO_x substrate, followed by evaporation of the Au source and drain electrodes through a shadow mask (chamber pressure = 10^{-6}mbar, evaporation rate = 0.05 nm/s). Finally, the devices were annealed at 60 °C for 1 h inside the glovebox to recover from moisture.

Electrical Characterization of the Devices. Electrical characterization of the devices was performed at room temperature in a N_2 atmosphere inside a glovebox, using a Cascade Microtech M150 probe station and a Keithley 2636A dual sourcemeter as semiconductor parameter analyzer controlled by associated software. Field-effect mobilities in single-fiber-based devices were estimated by determining the channel widths (W) and lengths (L) from the coverage in AFM images, whereas for multiple fiber devices optical microscopy images were used.

To study the photoresponse, devices were characterized under illumination from the top using a Leica LED1000 OLED ring (white light, 5.06 mW/cm^2) and an Optometric LLC TLS-25 M tunable light source providing a monochromatic beam with 580 nm wavelength and irradiance level of 7.24 μW/cm^2. The light intensity was measured using an analog optical power meter, PM100A (ThorLabs).

Instrumentation. UV−vis absorption measurements on PDI films drop-cast on quartz, from a 10^{-4} mol/L solution in $CHCl_3$, were carried out using a Shimadzu UV-3101PC. The same was applied for the deposition of the **1**−**3** fibers which were prepared as described above.

Atomic Force Microscopy (AFM) images were recorded using Nanoscope (Veeco Multimode V)

Measurements for the thickness of the active layer were performed using Alpha step IQ profiler.

RESULTS AND DISCUSSION

Characteristics in the Dark. Figure 1 displays transfer characteristics of 20-μm channel length **1**-based OFET incorporating in the channel either a spin-coated thin film (*tf-OFET*) (Figure 1b) or drop-cast fibers (*multifib-OFET*) (Figure 1c), with their output characteristics shown as insets. Both types of devices exhibit a typical n-type behavior. The field-effect mobility $\boldsymbol{\mu}$, was extracted from the saturation regime at V_D = 80 V. For the *multifib-OFETs*, due to the incomplete coverage of the channel (see inset Figure 1c) which results in a decrease of the effective channel width, $\boldsymbol{W}$, the mobilities were corrected by estimating the coverage on the basis of optical microscopy images. The extracted $\boldsymbol{\mu}$, V_T, and on/off ratio respectively amount to 1.27 × 10^{-3} cm^2/(V s), 23 V, and 10^5 for the *tf-OFET*, and 4.24 × 10^{-4} cm^2/(V s), 26 V, and 10^3 for the *multifib-OFET*. On the one hand, the lower on−off ratio obtained in *multifib-OFETs* as compared to that of the *tf-OFETs* is due to the greater thickness of the fibers (ranging from 300 nm up to 1.5 μm) when compared to that of the films (spanning from 40 nm up to 120 nm). On the other hand, the lower mobility observed in *multifib-OFETs* can be ascribed to the nonoptimal electrode−semiconductor interface generated upon deposition of previously formed SIP fibers on the electrodes. In fact, differently from spin-coated films, the deposition of previously formed SIP fibers does not involve a self-assembly phenomena on the electrodes. To solve this problem, we extended our studies to the use of top contact

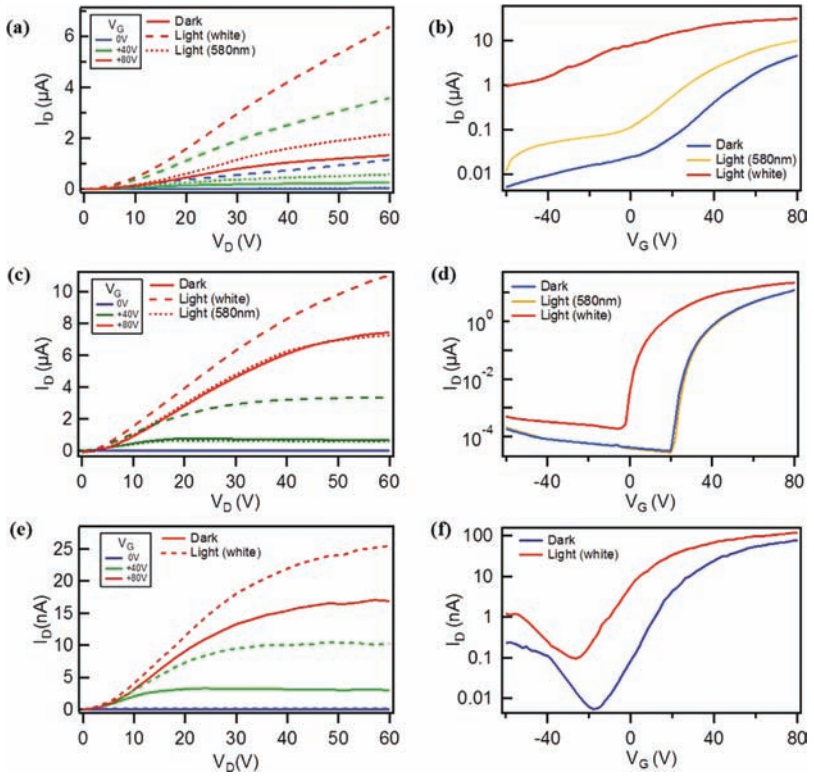

Figure 2. Comparison of (a) output and (b) transfer characteristics at V_D = 80 V of **1** *multifib-OPT*; (c) output and (d) transfer characteristics at V_D = 80 V of **1** *tf-OPT* with the same channel length L = 20 μm measured in dark, under white light and monochromatic light (λ = 580 nm); (e) output and (f) transfer characteristics at V_D = 80 V of **1** *monofib-OPT* (L = 14 μm) measured in dark and under white light.

geometry in OFETs incorporating a single macrofiber, being a bundle of smaller fibers.

The inset of Figure 1d (see also Figure S1 in the SI) shows the AFM image of such device having a channel length of 14 μm. The channel width is defined by the fiber's width of 0.56 μm, whereas the fiber's average height is 166 nm. The corresponding transfer characteristics are shown in Figure 1d. The field-effect mobility averaged on five devices amounts to 1.2×10^{-2} cm^2/(V s), being 1 order of magnitude higher than that of the *tf-OFET*, as a result of a better charge injection at the interface in a top contact device. This result is particularly relevant not only because in single-fiber-based devices neither the dielectric interface nor the source-drain electrodes were treated to improve wettability and charge injection, but also because the *monofib-OFET*, based on the air-unstable **1**, were exposed to air for a few hours during the sample preparation process involving the use of a mask to deposit top electrodes. Conversely, the *multifib-OFET* and *tf-OFET* were fabricated and characterized inside the glovebox, i.e. they were not exposed to air. It is fair to note that for transistors based on **1** and **2** higher μ were reported only in vacuum-processed devices.[3d,f,11]

Characteristics under Illumination. The difference in output and transfer characteristics of **1**-based *tf-OPT* (L = 20 μm) and *multifib-OPTs* (L = 20 μm) in dark and under illumination with white light (5.06 mW/cm^2) and monochromatic light (7.24 μW/cm^2) at λ = 580 nm is illustrated in Figure 2. This wavelength was chosen in view of the absorption characteristics of **1**−**3** (Figure S2 in the SI). Figure 2a,b shows the increase of the drain current in the I_D−V_D and I_D−V_G curves upon irradiation of the *multifib-OPT* with monochromatic light as a result of the photogeneration of excitons (i.e., electron−hole pair) that dissociate into free charge carriers which subsequently move toward the electrodes under the influence of the electric field. The ratio of the photocurrent to the dark current (I_{light}/I_{dark}) at V_G = 26 V was calculated to be ∼9, whereas it amounted to ∼140 (15 times higher) upon illumination with white light (Figure 2b). This results in a nonsaturation behavior of the I_D−V_D curves that was more remarkable with the increasing positive gate bias (Figure 2a). Such an observation can also be ascribed to the power of the used incident white light, being 3 orders of magnitude higher than that of the monochromatic light. The devices illuminated with white light could not be switched off efficiently at very low negative V_G (Figure 2b) under these high illumination conditions, as also observed in **2**-based *multifib-OPTs* (see Figure S3 in the SI). For this reason, we have focused our attention on bottom-contact fiber-based devices illuminated with monochromatic light. The *tf-OPTs* did not exhibit a clear photoresponse upon irradiation with monochromatic light, as shown in Figure 2c,d. This is most probably due to the polycrystalline nature of the semiconducting film hindering the efficient dissociation of the photogenerated excitons and their diffusion toward the electrodes, in line with recent observations that in PDI films the diffusion length of excitons is higher in ordered structures as compared to the film.[12] Conversely, under illumination with the more powerful white light I_D increases significantly (Figure 2c); the I_{light}/I_{dark} amounted to 6×10^3 at V_G = 23 V (Figure 2d). For this reason *tf-OPTs* were investigated only under white light.

Figure 2e shows that *monofib-OPTs* based on **1** under illumination with white light exhibit a significant photoresponse ($I_{light}/I_{dark} \approx 60$ at V_G = 2 V, Figure 2f). The average field-effect mobility was found to be unaffected by illumination,

dx.doi.org/10.1021/ja211515b | *J. Am. Chem.Soc.* 2012, 134, 2429−2433

whereas the threshold voltage was found to shift toward lower values. The latter observation was encountered also on *tf-OPTs* (Figure S4a) and *multifib*-OPTs (Figure S4b). The origin of the threshold voltage shift had been ascribed to (i) the large number of the photogenerated charge carriers trapped under the source, thus lowering the source-channel potential barrier,[13] (ii) the screening of the gate voltage by a built-in field resulting from the charges trapped at the interface with the dielectric,[3a] and (iii) the photogenerated current that increases the total current.[14]

All investigated PDI-based *tf-OPTs* exhibited high photosensitivity, ***P***, under white light illumination ranging from 10^3 to 10^7, indicating a pronounced increase of the signal upon irradiation. A maximum ***R*** value of 431 A/W with a corresponding ***P*** value of 1.34×10^6 was obtained for **1** *tf-OPT* with $L = 2.5$ μm. For *multifib-OPTs* of **1**−**3** irradiated with monochromatic light, the ***P*** values ranged from $\sim 10^1$ to 10^3, i.e. several orders of magnitude lower than that of *tf-OPT* due to the higher off-state and to the lower intensity of the employed light. In contrast ***R*** values of *multifib-OPTs* (corrected for coverage) were 2−3 orders of magnitude higher compared to the ones for *tf-OPTs*. The average ***R*** value obtained was $4.08 \pm 1.65 \times 10^5$ A/W for 2.5 μm channel length of **1** *multifib*-OPTs that is, to the best of our knowledge, the highest reported value to date.

Figure 3a,b shows the difference between the responsivity and the photosensitivity for the same channel length (L = 20 μm) and width (W = 10 mm) of a **1** *tf-OPT* and *multifib-OPT*, respectively. For **1** single-fiber OPT illustrated in the inset of Figure 1d, ***R*** and ***P*** values were, in turn, 118 A/W and 95 (Figure 3c).

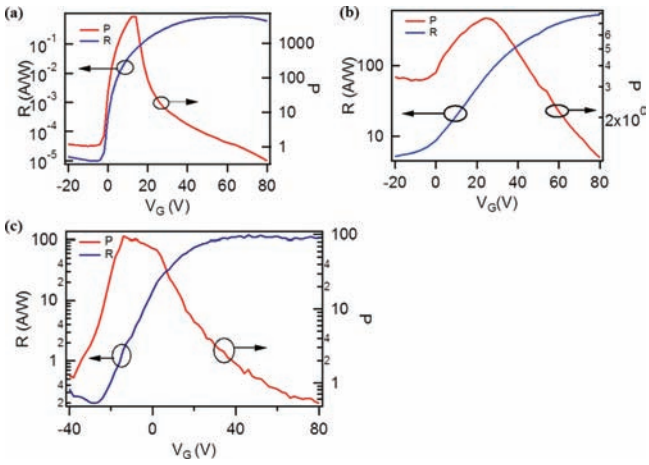

Figure 3. Variation of responsivity ***R*** and photosensitivity ***P*** with V_G at V_D = 80 V for **1**: (a) *tf-OPT* (L = 20 μm) under white light, (b) *multifib-OPT* (***L*** = 20 μm) under monochromatic light. (c) *monofib-OPT* (L = 14 μm).

The dependence of the responsivity ***R*** on the channel length for both **1**−**3** *tf-* and *multifib-OPTs* is depicted in a and b of Figure 4, respectively. The curves can be best fitted using a power law, in particular a −2 power, that can be derived at the saturation regime from the following:

$$I_D = \frac{W}{2L}\mu C_i (V_G - V_T)^2 = \frac{W}{2L}\mu C_i (V_{Geff})^2 \qquad (2)$$

where V_{Geff} is the effective gate voltage, V_G the gate voltage, V_T the threshold voltage, C_i the capacitance per unit area of the insulator layer, and all the other parameters were previously defined.

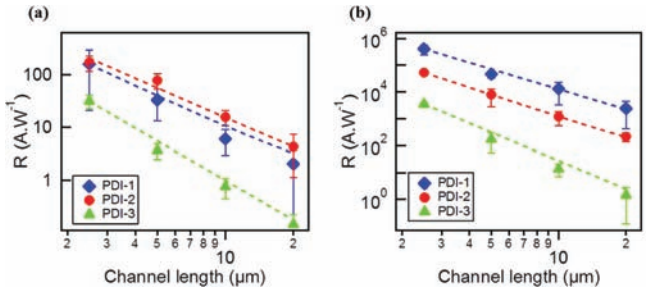

Figure 4. Dependence of the responsivity (**R**) on the channel length (**L**) for **1**−**3** based (a) *tf-OPTs* upon illumination with white light. (b) *multifib-OPT* upon illumination with monochromatic light, fitted (dashed lines) using a power law with a power of −2.

For a constant channel width, by substituting I_D in the equation for ***R*** (as previously defined)

$$R = \frac{I_L - I_D}{E \times A}$$

and assuming that the mobility is unchanged under illumination, eq 2 becomes:

$$R = \frac{\mu C_i}{2E \times L^2} \times (2V_{Geff}\Delta V_T + \Delta V_T{}^2) \qquad (3)$$

This gives a clear explanation of the increase of the responsivity by decreasing the channel length. The "−2" power law dependence of ***R*** on ***L*** indicates that the response can be tuned by the device geometry. The small deviation from the "−2" power law fitting can be due to the accumulation of charge carriers under the electrodes resulting in a decrease of the contact resistance.

A close look at the graphs in Figure 4a reveals that for *tf-OPTs* based on **1** and **2** exhibited similar responsivity which is much higher than for **3**. This difference could be resulting from the role of the side chains influencing the $\pi-\pi$ stacking through steric effects, thus affecting the photoresponse. It was shown that thin film of **1** and **2** exposing linear alkyl chains pack similarly in thin films[3d] which is reflected in their similar photoresponse. On the other hand, the presence of branched side chains in molecule **3** hinders $\pi-\pi$ stacking, leading to a lower responsivity. Conversely, *multifib-OPTs* of **1** (Figure 4b) exhibited the highest responsivity when illuminated with monochromatic light. It is important to mention that the band gaps of **1**−**3** are basically identical since the lengths of the alkyl substituents at the imide nitrogen do not induce significant alteration of electronic properties of the PDI molecule.[15]

■ CONCLUSION

In summary, we found that the responsivity to light illumination in solution-processed PDI-based OPTs depends on the channel length. Our results suggest that the photoresponse in OPTs can be tuned by varying the device geometry and the morphology of the active semiconducting layer, revealing that single fibers possess the higher response when compared to more poorly organized films. Taking advantage of these findings we have realized a PDI multifiber-based OPT featuring a record responsivity value of $4.08 \pm 1.65 \times 10^5$ A/W. Our results represent a step forward toward the possible use of

dx.doi.org/10.1021/ja211515b | J. Am. Chem.Soc. 2012, 134, 2429−2433

these devices as photosensors in optoelectronics, where light can act as an additional control parameter.

■ ASSOCIATED CONTENT

Supporting Information

Further details about the absorption spectra, electrical characteristics upon illumination of the devices. This material is available free of charge via the Internet at http://pubs.acs.org.

■ AUTHOR INFORMATION

Corresponding Author

samori@unistra.fr

■ ACKNOWLEDGMENTS

We thank Dr. Emanuele Orgiu for his comments on the manuscript. This work was supported by the ERC project SUPRAFUNCTION (GA-257305). The Strasbourg−Mainz collaboration is supported by EC through the FP7 ONE-P Large-Scale Project no. 212311, the Marie-Curie ITN-GENIUS (PITN-GA-2010-264694) and ITN-SUPERIOR (PITN-GA-2009-238177), and the NanoSci-E+ Project SENSORS. Supports from the International Center for Frontier Research in Chemistry (FRC) are also gratefully acknowledged.

■ REFERENCES

(1) (a) Würthner, F. *Chem Commun* **2004**, 1564. (b) Anthony, J. E.; Facchetti, A.; Heeney, M.; Marder, S. R.; Zhan, X. W. *Adv. Mater.* **2010**, *22*, 3876. (c) Jones, B. A.; Ahrens, M. J.; Yoon, M. H.; Facchetti, A.; Marks, T. J.; Wasielewski, M. R. *Angew. Chem., Int. Ed.* **2004**, *43*, 6363. (d) Nolde, F.; Qu, J. Q.; Kohl, C.; Pschirer, N. G.; Reuther, E.; Müllen, K. *Chem.—Eur. J.* **2005**, *11*, 3959. (e) Nolde, F.; Pisula, W.; Muller, S.; Kohl, C.; Müllen, K. *Chem. Mater.* **2006**, *18*, 3715. (f) Elemans, J. A. A. W.; Van Hameren, R.; Nolte, R. J. M.; Rowan, A. E. *Adv. Mater.* **2006**, *18*, 1251.

(2) Horowitz, G.; Kouki, F.; Spearman, P.; Fichou, D.; Nogues, C.; Pan, X.; Garnier, F. *Adv. Mater.* **1996**, *8*, 242.

(3) (a) Barra, M.; Bloisi, F.; Cassinese, A.; Di Girolamo, F. V.; Vicari, L. *J. Appl. Phys.* **2009**, *106*, 126105. (b) Briseno, A. L.; Mannsfeld, S. C. B.; Reese, C.; Hancock, J. M.; Xiong, Y.; Jenekhe, S. A.; Bao, Z.; Xia, Y. *Nano Lett.* **2007**, *7*, 2847. (c) Chen, F. C.; Liao, C. H. *Appl. Phys. Lett.* **2008**, *93*, 103310. (d) Chesterfield, R. J.; McKeen, J. C.; Newman, C. R.; Ewbank, P. C.; Da Silva Filho, D. A.; Brédas, J. L.; Miller, L. L.; Mann, K. R.; Frisbie, C. D. *J. Phys. Chem. B* **2004**, *108*, 19281. (e) Jeon, H. G.; Hattori, J.; Kato, S.; Oguma, N.; Hirata, N.; Taniguchi, Y.; Ichikawa, M. *J. Appl. Phys.* **2010**, *108*, 124512. (f) Malenfant, P. R. L.; Dimitrakopoulos, C. D.; Gelorme, J. D.; Kosbar, L. L.; Graham, T. O.; Curioni, A.; Andreoni, W. *Appl. Phys. Lett.* **2002**, *80*, 2517. (g) Struijk, C. W.; Sieval, A. B.; Dakhorst, J. E. J.; Van Dijk, M.; Kimkes, P.; Koehorst, R. B. M.; Donker, H.; Schaafsma, T. J.; Picken, S. J.; Van de Craats, A. M.; Warman, J. M.; Zuilhof, H.; Sudholter, E. J. R. *J. Am. Chem. Soc.* **2000**, *122*, 11057. (h) Tatemichi, S.; Ichikawa, M.; Koyama, T.; Taniguchi, Y. *Appl. Phys. Lett.* **2006**, *89*, 112108. (i) Wen, Y.; Liu, Y.; Di, C. A.; Wang, Y.; Sun, X.; Guo, Y.; Zheng, J.; Wu, W.; Ye, S.; Yu, G. *Adv. Mater.* **2009**, *21*, 1631.

(4) (a) Cotlet, M.; Masuo, S.; Luo, G. B.; Hofkens, J.; Van der Auweraer, M.; Verhoeven, J.; Müllen, K.; Xie, X. L. S.; De Schryver, F. *Proc. Nat. Acad. Sci. U.S.A.* **2004**, *101*, 14343. (b) De Schryver, F. C.; Vosch, T.; Cotlet, M.; Van der Auweraer, M.; Müllen, K.; Hofkens, J. *Acc. Chem. Res.* **2005**, *38*, 514.

(5) (a) Dittmer, J. J.; Lazzaroni, R.; Leclère, P.; Moretti, P.; Granström, M.; Petritsch, K.; Marseglia, E. A.; Friend, R. H.; Brédas, J. L.; Rost, H.; Holmes, A. B. *Sol. Energy Mater. Sol. Cells* **2000**, *61*, 53. (b) Würthner, F.; Chen, Z. J.; Hoeben, F. J. M.; Osswald, P.; You, C. C.; Jonkheijm, P.; von Herrikhuyzen, J.; Schenning, A.; van der Schoot, P.; Meijer, E. W.; Beckers, E. H. A.; Meskers, S. C. J.; Janssen, R. A. J. *J. Am. Chem. Soc.* **2004**, *126*, 10611. (c) Li, J. L.; Dierschke, F.; Wu, J. S.; Grimsdale, A. C.; Müllen, K. *J. Mater. Chem.* **2006**, *16*, 96. (d) Palermo, V.; Otten, M. B. J.; Liscio, A.; Schwartz, E.; de Witte, P. A. J.; Castriciano, M. A.; Wienk, M. M.; Nolde, F.; De Luca, G.; Cornelissen, J. J. L. M.; Janssen, R. A. J.; Müllen, K.; Rowan, A. E.; Nolte, R. J. M.; Samorì, P. *J. Am. Chem. Soc.* **2008**, *2008*, 14605. (e) Shin, W. S.; Jeong, H. H.; Kim, M. K.; Jin, S. H.; Kim, M. R.; Lee, J. K.; Lee, J. W.; Gal, Y. S. *J. Mater. Chem.* **2006**, *16*, 384. (f) Liscio, A.; De Luca, G.; Nolde, F.; Palermo, V.; Müllen, K.; Samorì, P. *J. Am. Chem. Soc.* **2008**, *130*, 780.

(6) Guo, Y.; Yu, G.; Liu, Y. *Adv. Mater.* **2010**, *22*, 4427.

(7) Saragi, T. P. I; Onken, K.; Suske, I.; Fuhrmann-Lieker, T.; Salbeck, J. *Opt. Mater.* **2007**, *29*, 1332.

(8) Kim, K. H.; Bae, S. Y.; Kim, Y. S.; Hur, J. A.; Hoang, M. H.; Lee, T. W.; Cho, M. J.; Kim, Y.; Kim, M.; Jin, J.-I.; Kim, S.-J.; Lee, K.; Lee, S. J.; Choi, D. H. *Adv. Mater.* **2011**, *23*, 3095.

(9) Guo, Y.; Du, C.; Yu, G.; Di, C.-a.; Jiang, S.; Xi, H.; Zheng, J.; Yan, S.; Yu, C.; Hu, W.; Liu, Y. *Adv. Funct. Mater.* **2010**, *20*, 1019.

(10) Sakamoto, T.; Pac, C. *J. Org. Chem.* **2001**, *66*, 94.

(11) Yoo, B.; Jung, T.; Basu, D.; Dodabalapur, A.; Jones, B. A.; Facchetti, A.; Wasielewski, M. R.; Marks, T. J. *Appl. Phys. Lett.* **2006**, *88*, 082104.

(12) Lunt, R. R.; Benziger, J. B.; Forrest, S. R. *Adv. Mater.* **2010**, *22*, 1233.

(13) (a) Hamilton, M. C.; Kanicki, J. *IEEE J. Sel. Top. Quantum Electron.* **2004**, *10*, 840. (b) Hamilton, M. C.; Martin, S.; Kanicki, J. *IEEE Trans. Electron Devices* **2004**, *51*, 877. (c) Marjanovic, N.; Singh, T. B.; Dennler, G.; Günes, S.; Neugebauer, H.; Sariciftci, N. S.; Schwödiauer, R.; Bauer, S. *Org. Electron.* **2006**, *7*, 188.

(14) Wasapinyokul, K. *J. Appl. Phys.* **2011**, *109*, 084510.

(15) Ruiz Delgado, M. C.; Kim, E.-G.; da Silva Filho, D. A.; Brédas, J.-L. *J. Am. Chem. Soc.* **2010**, *132*, 3375.